

The fourth quadrant in the ϵ , μ plane: A new frontier in optics

E. N. Economou^{1,2,*}, M. Kafesaki^{1,3}, C. M. Soukoulis^{1,3,4}, Th. Koschny^{1,4}

¹*Foundation for Research and Technology Hellas (FORTH), Institute of Electronic Structure and Laser (IESL), P.O. Box 1385, 71110 Heraklion, Crete, Greece*

²*University of Crete, Department of Physics, Heraklion Crete, Greece*

³*University of Crete, Department of Materials Science and Technology, Greece*

⁴*Iowa State University – Ames Lab and Physics Department, Ames, Iowa, USA*

**Corresponding author. Tel: +302810 391565, Fax: +30 2810 391569,*

economou@admin.forth.gr

Abstract. We review and analyze some of the novel and unique characteristics of the electromagnetic wave propagation in materials of both negative electrical permittivity and magnetic permeability, known as left-handed materials. Main steps and recent developments towards the realization and exploitation of such materials are described, while emphasis is given to the attempts for “extension” of left-handed materials towards the optical regime. There, some of the main advances and challenges are analyzed and discussed.

Keywords: left-handed materials, metamaterials, negative refractive index

Table of Contents

I. Introduction	2
II. EM waves in a medium where $\mu < 0$ and $\epsilon < 0$	4
III. Designing and fabricating LHMs	7
IV. Measuring LHMs	9
V. Goals and problems	11
VI. Summary	14
References	15

I. Introduction

Electromagnetic (EM) waves as carriers of information and energy are of central importance in our lives from biological, technological, and scientific points of view. Thus: Energy and information (negentropy) is transferred from the Sun to the Earth through EM waves, providing the necessary requirements for the development and sustaining of living organisms. Various objects are visible because they reflect EM waves which in turn are processed in our eyes, in the optical nerves and finally in our brains. Telecommunication devices (radios, TVs, mobile telephones, etc) are connected through EM waves. Medical information regarding the functioning (and malfunctioning) of various organs are obtained through EM waves (MRI, X-ray tomography, etc). Tremendous amount of information about the present state and the history of the Cosmos beyond our planet are collected again by EM waves from the radio frequencies to X-rays and beyond.

To employ EM waves it is necessary to have properly assembled matter (biologically or technologically) which, through its interaction with EM waves, can emit, receive, store, process, and allow retrieval of information and energy. Hence there is a never ending quest for new forms of matter (or combinations of existing materials) beyond those which nature and present day technology offers us.

It is worthwhile to point out that the interaction of EM waves with matter (in all its forms) takes place almost exclusively through the electric component of the electromagnetic field; the magnetic component of the EM field does not produce usually an appreciable response. This is so because the force exercised on a charged particle by the magnetic component of the field is of the order v/c relative to that of the electric component, where v is the velocity of the particle and c is the velocity of light in the vacuum. As a result, the response of a material to the magnetic field as measured by the magnetic susceptibility, χ , is of the order of $v^2/c^2 \sim 10^{-5}$. One way to beat this intrinsic small factor is to have a collective response, as, e.g., in ferromagnets; however, even in this case the strong response dies out as the frequency of the EM field is raised beyond a few tens of a GHz. Another way to have a strong magnetic response is to operate under strong resonance conditions, which may produce a χ vs. ω dependence as shown in Fig. 1.

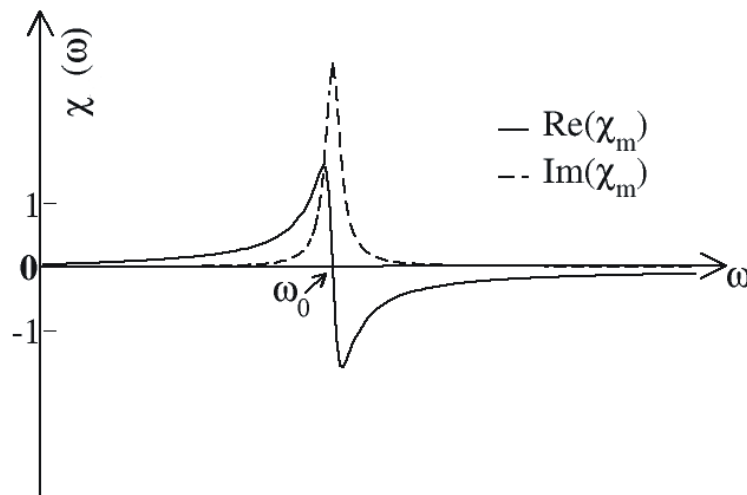


Fig. 1. Typical resonance response of the real and imaginary part of the magnetic susceptibility vs. frequency. At the resonance frequency, ω_0 , $\text{Im}\chi$ has a maximum and $\text{Re}\chi$ passes through zero.

If the losses associated with the resonance are very small the peak of the $Im\chi$ becomes very narrow and the absolute value of the maximum and the minimum of the $Re\chi$ becomes very large, even larger than one. In this case the real part of the relative permeability $\mu \equiv \hat{\mu}/\mu_o = 1 + \chi$ can take values around the resonance ranging from larger than two to smaller than zero ($\hat{\mu}$ is the magnetic permeability and μ_o is the permeability of the vacuum).

Keeping in mind this possibility of strong magnetic response, let us return to the electric response of a homogeneous material, which is mainly characterized by the so called dielectric function or relative permittivity, $\epsilon \equiv \hat{\epsilon}/\epsilon_o$, where $\hat{\epsilon}$ is the permittivity and ϵ_o is the vacuum permittivity; ϵ is in general a function of both the frequency, ω , and the wavenumber, k , (for a homogeneous and isotropic medium) and it has a real and an imaginary part. For a non-polar dielectric ϵ is larger than one and usually almost constant up to frequencies in the near ultraviolet. For metals the dielectric function is of the form^{1,2}

$$\epsilon(\omega) = \epsilon^{(0)} \left(1 - \frac{\omega_p^2}{\omega^2 + i\omega/\tau} \right), \quad (1)$$

where $\epsilon^{(0)} = 1 + \epsilon_b$, and ϵ_b is the contribution of strongly bound electrons; $\omega_p^2 = e^2 n_e / m_e \epsilon_o \epsilon^{(0)}$, where n_e is the concentration of “free” electrons, m_e is the electron mass and τ is the relaxation time.

The phase velocity of EM waves in a homogeneous medium characterized by ϵ and μ is given by

$$v_p \equiv \frac{\omega}{k} = \frac{c}{n}; \quad n = \sqrt{\epsilon\mu}. \quad (2)$$

For a typical dielectric ϵ is positive and larger than one, μ is very close to one, the index of refraction, n , is positive and larger than one, and v_p is smaller than c . For a metal and for $\omega < \omega_p$, $\epsilon(\omega) < 0$, μ is usually almost one, $\epsilon\mu$ is negative, n is imaginary and the EM waves decay exponentially with a characteristic length^{2, 3, 4} $\ell_d = c / \sqrt{|\epsilon|} \omega$. These characteristic cases are summarized in Fig. 2.

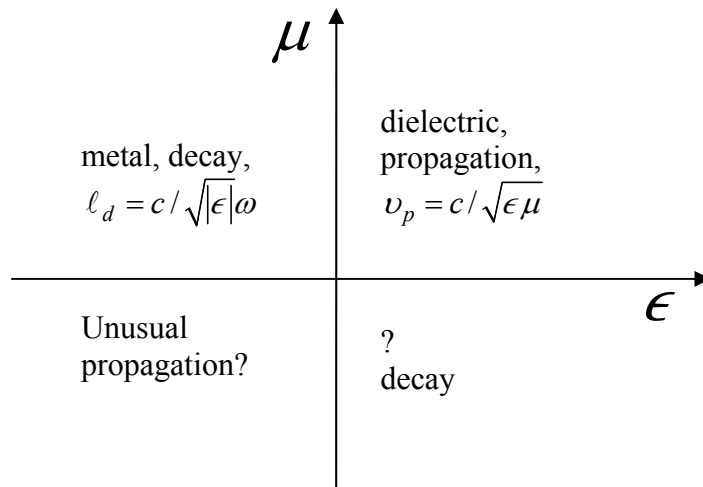


Fig. 2. Omitting the $Im\epsilon$ and $Im\mu$, the ϵ, μ plane is separated in four quadrants. The third one ($\mu < 0, \epsilon > 0$), even if it is realized, leads to decay, and hence, it presents no interest from the point of

view of optics. The fourth quadrant ($\mu < 0$, $\epsilon < 0$), for which $\epsilon\mu > 0$, allows propagation, possibly, a novel one⁵.

II. EM waves in a medium where $\mu < 0$ and $\epsilon < 0$

By writing the components of the EM field as²

$$\mathbf{E}(\mathbf{r}, t) = \frac{1}{\sqrt{2}} \mathbf{E}_o \exp(i\mathbf{k} \cdot \mathbf{r} - i\omega t) + c.c., \quad (3)$$

$$\mathbf{H}(\mathbf{r}, t) = \frac{1}{\sqrt{2}} \mathbf{H}_o \exp(i\mathbf{k} \cdot \mathbf{r} - i\omega t) + c.c., \quad (4)$$

we obtain from the Maxwell curl equations that

$$\mathbf{k} \times \mathbf{E} = \omega\mu\mu_o \mathbf{H}, \quad (5)$$

$$\mathbf{k} \times \mathbf{H} = -\omega\epsilon\epsilon_o \mathbf{E}. \quad (6)$$

Eqs. (5) and (6) show that the system \mathbf{k} , \mathbf{E} , \mathbf{H} is left-handed (LH) if μ and ϵ are negative⁵, while it is right-handed (RH) in the usual case where ϵ and μ are positive.

By cross multiplying (5) by $\mathbf{E} \times$ and (6) by $\mathbf{H} \times$ and by time averaging, we have

$$\mathbf{k} = \frac{\omega\mu\mu_o}{E_o^2} \mathbf{E}_o \times \mathbf{H}_o = \frac{\omega\epsilon\epsilon_o}{H_o^2} \mathbf{E}_o \times \mathbf{H}_o, \quad (7)$$

from which it follows that

$$\frac{E_o^2}{\mu\mu_o} = \frac{H_o^2}{\epsilon\epsilon_o}. \quad (8)$$

The time-averaged energy flux density, \mathbf{S} , is given either by the product $u\mathbf{v}_g$, where u is the time-averaged energy density and \mathbf{v}_g is the group velocity^{*}, or by the time-averaged Poynting vector,

$$\mathbf{S} = u\mathbf{v}_g = \mathbf{E}_o \times \mathbf{H}_o. \quad (9)$$

By combining (7) and (9) we obtain

$$\mathbf{k} = \frac{\omega\mu\mu_o}{E_o^2} \mathbf{S} = \frac{\omega\epsilon\epsilon_o}{H_o^2} \mathbf{S}, \quad (10)$$

$$\mathbf{k} = \frac{\omega\mu\mu_o}{E_o^2} u \mathbf{v}_g = \frac{\omega\epsilon\epsilon_o}{H_o^2} u \mathbf{v}_g. \quad (11)$$

Eqs. (10) and (11) show that the propagation of phase, as determined by \mathbf{k} , is in the opposite direction of the propagation of energy, as determined by \mathbf{S} or \mathbf{v}_g (since μ and ϵ are negative), or, equivalently, \mathbf{v}_p and \mathbf{v}_g are opposite to each other.

An immediate consequence of (10) and (11), combined with the conservation of the parallel component of \mathbf{k} at a planar interface, is that the refraction at such an interface between a material with ϵ, μ positive and a material with ϵ, μ negative is as shown in Fig. 3. Hence, when $\epsilon, \mu < 0$, the index of refraction n must be the negative square root of $\epsilon\mu$: $n = -\sqrt{\epsilon\mu}$.

^{*} Providing not strong resonance conditions, such that the group velocity represents the velocity of the energy propagation.

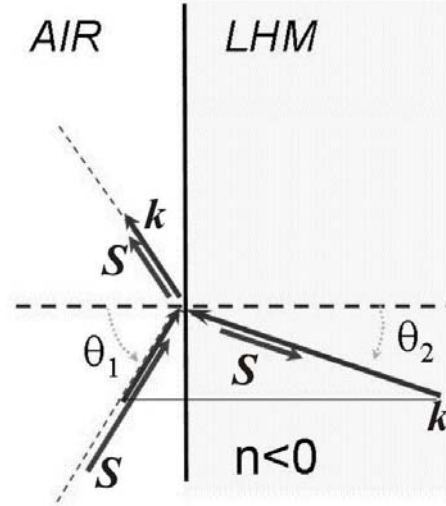


Fig. 3. Reflection and refraction at the interface of a right-handed material ($\epsilon, \mu > 0$), like air, and a left-handed one ($\epsilon, \mu < 0$). The conservation of the parallel component of \mathbf{k} in combination with Eq. (10) or (11) leads to a negative value of θ_2 , satisfying Snell's law, $n_1 \sin \theta_1 = n_2 \sin \theta_2$, with n_2 (n in the figure) negative.

From the equations (3) to (11) one can show that^{3, 4}

$$\mathbf{v}_g = \frac{\mathbf{v}_p}{1 + (\omega/n)(\partial n/\partial \omega)}, \quad (12)$$

$$u = \frac{1}{2} \left[\frac{\partial(\omega \epsilon \epsilon_o)}{\partial \omega} E_o^2 + \frac{\partial(\omega \mu \mu_o)}{\partial \omega} H_o^2 \right], \quad (13)$$

$$\mathbf{p} = \frac{\epsilon \mu}{c^2} \mathbf{S} + \frac{\mathbf{k}}{2} \left[\frac{\partial \epsilon}{\partial \omega} \epsilon_o E_o^2 + \frac{\partial \mu}{\partial \omega} \mu_o H_o^2 \right], \quad (14)$$

where \mathbf{p} is the time-averaged momentum density. To obtain (14) we have used also the relativistic equation $u = v_p p$, connecting the energy density, u , with the momentum density, p .

This brief analysis shows that EM wave propagation in a medium with both ϵ and μ negative exhibits novel and unexpected features, such as⁵:

- The triad \mathbf{k} , \mathbf{E} , \mathbf{H} is left-handed.
- Phase and energy propagate in opposite directions.
- The index of refraction is negative^{5, 6}, $n = -\sqrt{\epsilon \mu}$.
- The refraction angle is negative according to Snell's law, $n_1 \sin \theta_1 = n_2 \sin \theta_2$ (where θ_2 is the refraction angle and $n_2 < 0$) (see Fig. 3).
- If $n_2 \approx 0$, then $\theta_1 = 0$ (see Snell's law above), which means that a directed beam can be created out of any source located at a LH material with $n_2 \approx 0$ (see Fig. 4).
- In a LH material the Doppler effect is opposite, i.e. blue shift occurs if the source is moving away from the detector.
- Opposite Cherenkov radiation: The energy flow is opposite to \mathbf{k} ; the latter makes an angle $\theta (< 90^\circ)$ with the velocity of the particle, \mathbf{v} , such that $\cos \theta = c/|n|v$.
- Opposite radiation pressure, \mathbf{P} : $\mathbf{P} = 2u\mathbf{k}_o$, $\mathbf{k}_o = \mathbf{k}/|\mathbf{k}|$, so that \mathbf{P} is opposite to the energy flow.

(i) Flat lense capability, as shown in Fig. 5.

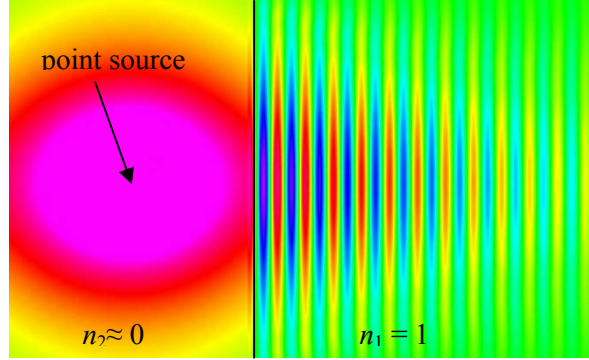


Fig. 4. A point source within a material of $n_2 \approx 0$ produces an almost plane wave in a material with $n_1 = 1$ according to the Finite Difference Time Domain simulation presented here.

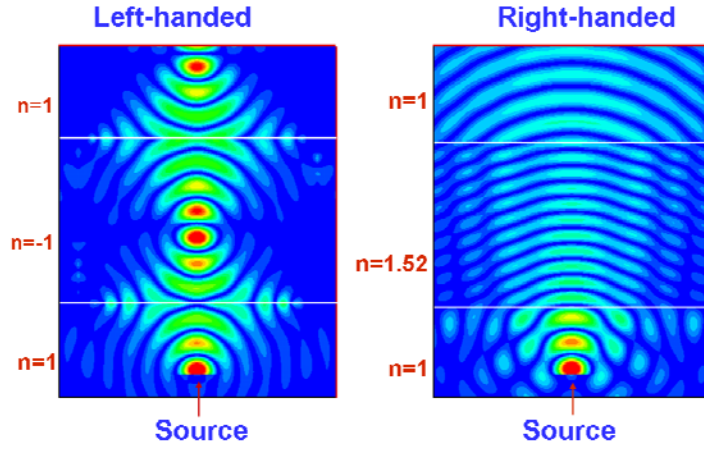


Fig. 5. Propagation of EM wave emitted from a point source and passing through a flat LH slab of $n = -1$ (left panel) or through a flat RH slab of $n = 1.52$ (glass - right panel). In the LH case there is a focus inside the material and a focus on the other side.

(j) Perfect lenses. Consider an object emitting (or reflecting) EM waves which can be analyzed in Fourier components as

$$\mathbf{E}(\mathbf{r}, t) = \sum_{\mathbf{q}, \sigma} \mathbf{E}_{\sigma, \mathbf{q}} e^{i\mathbf{q} \cdot \mathbf{R} + ik_z z - i\omega t}, \quad (15)$$

where $\mathbf{q} = q_x \mathbf{i} + q_y \mathbf{j}$, $\mathbf{R} = x\mathbf{i} + y\mathbf{j}$, $k_z = \sqrt{(\omega^2/c^2) - q^2}$, and σ is the polarization index. If $q > \omega/c$, k_z becomes imaginary and $\exp(ik_z z) = \exp(-|k_z|z)$; thus as z increases the components with $q > q_o \equiv \omega/c$ (i.e. the evanescent waves) decay and the information they carry tends to disappear. At the far field, where $\exp(-|k_z|z) \approx 0$, the spatial resolution cannot be better than $2\pi/q_o = 2\pi c/\omega = \lambda$. On the other hand, inside a LHM where k_z is of opposite sign than S_z , it is reasonable to expect that instead of a decaying wave we have a growing wave, $\exp(+|k_z|z)$ for $q > q_o = \omega/c$. Detailed calculations, presented in Ref. 7, confirm this expectation. Thus, the evanescent waves are growing as they pass through a LHM. In particular, for a LHM with $\epsilon = \mu = n = -1$ of thickness $d = SA + BF$, where $SA + BF$ is the distance traveled by the EM wave in air between the source, S , and the focus, F , the evanescent wave will reach the focus without any

attenuation. Of course, practical considerations will limit the performance of this hypothetical perfect lens^{8,9}: Unavoidable losses in the LHM will lead to absorption and, hence, to a partial loss of information. To keep $\epsilon = \mu = n = -1$ over a wide frequency range (associated with a wave packet) may not be possible. Another objection that may be raised is the following: How a passive medium can amplify the EM wave? This apparent paradox can be understood by noticing that an evanescent wave in an infinite medium does not have a steady state propagation; nevertheless it can accumulate increased energy by increasing the time to approach its steady state condition. In other words, the increased energy accumulation is due to the time delay it takes for an EM wave to pass through a LH slab; thus energy is conserved.

III. Designing and fabricating LHMs

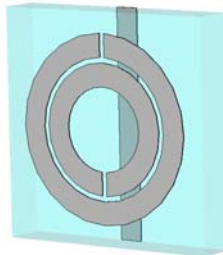
Conceptually, a way to create a LHM is to properly merge structures exhibiting negative $\text{Re}\epsilon$ with structures exhibiting negative $\text{Re}\mu$ at an overlapping frequency range¹⁰. This merging of negative $\text{Re}\epsilon$ and negative $\text{Re}\mu$ structures occurs at the level of elementary units, the so called “optical atoms”, which in turn are repeated periodically in space. If one wants to push the analogy with the ordinary condensed matter (which is made out of close-packed atoms), the size, a , of each “optical atom” must be much smaller than the average wavelength, λ , corresponding to the frequency range in which $\text{Re}\epsilon$ and $\text{Re}\mu$ are negative. This inequality, $a \ll \lambda$, is desirable (but not “sine qua non”), since it allows us to treat the LHM as an effective uniform medium which exhibits the desired property of negative index of refraction over a finite frequency range.

As it is clear from Eq. (1), metals provide an obvious choice for obtaining negative $\text{Re}\epsilon$; moreover ω_p can be “tuned” by using parallel “infinite” metallic wires periodically placed, instead of bulk metal¹¹. Indeed, one can show, by equating the average electric energy to the average magnetic energy due to an AC current flowing in the wires, that

$$\omega_p^2 \approx \frac{c^2}{a^2} \frac{4\pi}{\ln(a^2/s_o)} \quad (16)$$

where a^2 is the area per wire, and s_o is the geometrical cross-section of each wire.

Far from trivial is the design of the elementary subunit which will provide a resonant response to the magnetic field strong enough to drive $\text{Re}\mu$ to negative values. Pendry came up with the idea of a double split ring resonator¹² (SRR), shown in Fig. 6.



unit cell

Fig. 6. The metallic double split ring resonator (SRR) combined with a continuous metallic wire (on the back side of a dielectric) make up the unit cell of a LHM.

It was shown later on^{13, 14} that a single SRR (instead of a double one) with one or more cuts provides also a strong enough resonant response. Indeed, if the magnetic field is perpendicular to the plane of the SRR, it induces an electromotive force $-d\Phi/dt = -L_m(dI/dt)$ which drives a current around the ring; Φ is the magnetic flux through the ring, L_m is the self-inductance and I is the current. Because of the cut(s), charge is accumulated there, so that the cut(s) act as capacitors. Hence the SRR is an effective capacitor-inductor circuit, which has a resonant frequency $\omega_o = 1/\sqrt{L_m C}$, where C is the effective capacitance of the split ring. Notice that both L_m and C are proportional to the linear dimensions of the SRR^{13, 15}, or to the corresponding unit cell size, a , so that the resonance frequency ω_o (and, hence, the average frequency over which μ is negative) is proportional to $1/a$:

$$\omega_o \sim \frac{1}{a}. \quad (17)$$

This relation does not hold for very small a , because eventually the kinetic energy of the current carrying electrons, $\frac{1}{2}N_e m_e v^2 = \frac{1}{2}(\ell'/s\omega_p^2\epsilon_o\epsilon^{(o)})I^2$, where ℓ' is the effective length of the perimeter of the SRR and s is the cross-section of the SRR ring, ceases to be negligible; this is so because the effective inductance^{16, 15} $L_e = \ell'/s\omega_p^2\epsilon_o\epsilon^{(o)}$ of the electronic kinetic energy is proportional to $\ell'/s \sim 1/a$; thus

$$\omega_o \sim \frac{1}{\sqrt{a(a + A/a)}} = \frac{1}{\sqrt{a^2 + A}}, \quad (18)$$

where $A = L_e a^2 / L_m$. This dependence on the size (linear in a^{-1} for $a^2 \gg A$ and saturation for $a^2 \ll A$) is confirmed by both simulations^{15, 17} (see Fig. 7) and experiments¹⁸.

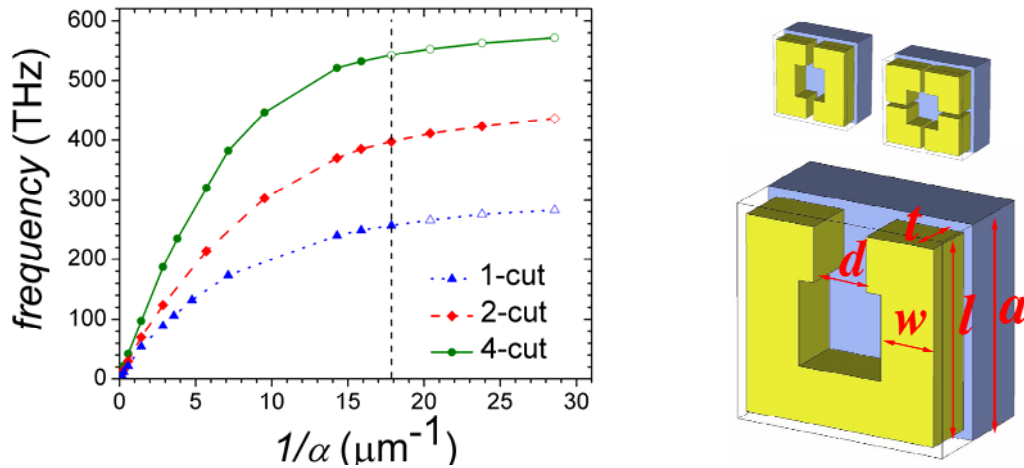


Fig. 7. Magnetic resonance frequency f_m vs. the inverse size a of the unit cell for a single SRR with 1, 2, and 4 cuts. (The corresponding designs are shown at the right-hand side of the figure, where the single-cut SRR is magnified as to make visible the characteristic SRR lengths). Dotted extensions of the lines indicate that the resonance is not strong enough to drive μ to negative values. The visible frequencies range is from 400 THz (red) to 750 THz (violet). The saturation value is given approximately by the following formula: $\omega_o = \sqrt{\epsilon^{(o)}} \omega_p \{1.8nd / [4(\ell - w) - nd]\}^{1/2}$, where n is the number of cuts, all of size d , ℓ is the length of each side of the SRR, and w is the ring-width.

In Fig. 8 we show how the two gap/cut SRR can be transformed to produce other designs¹⁹ till the so called fishnet design^{20, 21, 22} which seems to be the most successful one for achievement of left-handed behavior in both microwaves and optical regime.

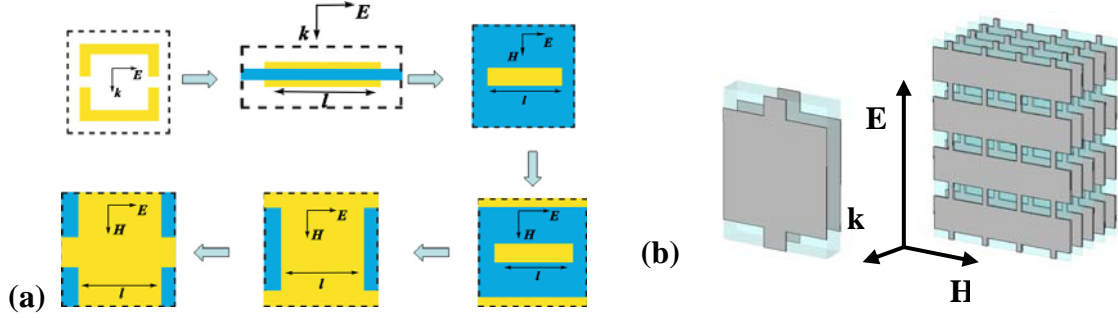


Fig. 8. (a): The two gap single-ring SRR can be transformed to that of two metal slabs (yellow color) separated by a dielectric (blue color) seen from the side and from the top. The two slab design can be reinforced with a pair of “infinite” wires on each side (lower right). Finally the width of the slabs can be increased as to join the parallel wires and thus to give rise to the fishnet design (two views of the unit cell are shown in the lower panel). (b): Three-dimensional view of the fishnet design: One unit cell (left) and multiple unit cells (right).

When combining within the unit cell the two elementary subunits (e.g. wire plus SRR), we have to take into account that the magnetic subunit (e.g. the SRR) exhibits electric response as well, since it behaves as a finite wire in the direction parallel to the electric field²³. The dielectric function of a metal wire of finite length is of the form

$$\epsilon(\omega) = \epsilon^{(0)} \left(1 - \frac{\omega_p^2}{\omega^2 - \omega_e^2 + i\omega/\tau} \right). \quad (19)$$

Thus the combined electric response of infinite metallic wires and SRRs (acting as finite wires as well) is as in the right panel of Fig. 9.

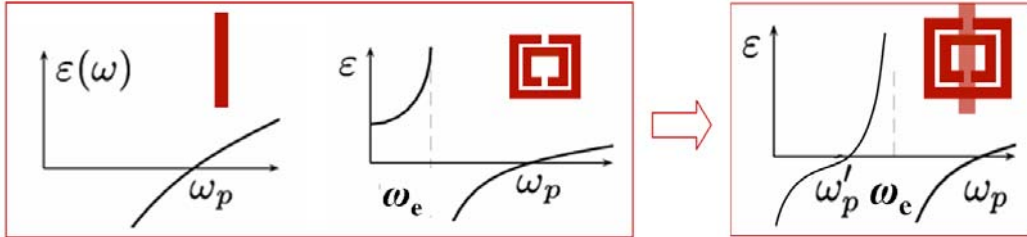


Fig. 9. Figure shows how the dielectric function of a system of continuous wires (left-panel), combined with the dielectric function of a system of SRRs or short wires (middle panel), result to the more complicated electric response of the composite SRRs&wires system (right panel).

IV. Measuring LHMs

There are two basic ways for confirming experimentally that LHMs have been actually realized. One is based on the negative refraction effect (see Fig.3), which can be facilitated by fabricating a wedge-like LHM; an EM wave of appropriate frequency enters the material from one side at normal incidence and exits from the other side of the wedge-like LHM at an oblique angle, which, depending on its sign relative to the normal, determines whether the material is LH or RH^{25, 26}. Recently, the Berkley group used this technique to demonstrate LH behavior in a stack of fishnets²⁷ at the near infrared, $\lambda = 1763$ nm.

The other way to confirm LH behavior is to measure the transmission through a flat slab of LHM and to identify frequency region(s) where a transmission peak appears

associated with $\epsilon(\omega)$ and $\mu(\omega)$ being both negative. To make sure that the observed peak is indeed LH, one must show that by eliminating the magnetic resonance²⁸ (e.g., by closing the gaps in SRRs) the peak disappears (since the closing of the gap changes μ from negative values to $\mu \approx 1$ and hence $n = \sqrt{\epsilon\mu}$ changes from real to imaginary).

Regarding the measuring/identification of the negative permeability regime in only-SRR structures, a worth-mentioning approach, extremely convenient in micro- and nano-scale structures, is by employing the so called excitation of the magnetic resonance by the electric field (EMREF)²⁹: Consider a configuration where the electric field is parallel to the gap bearing side of a single gap SRR; because of the asymmetry, the electric field induces a loop-like oscillatory current in the SRR which exhibits a resonance behavior when $\omega = \omega_o$, manifested as a dip in the SRR transmission spectra. On the other hand, if the electric field is parallel to the sides bearing no gap, no current is induced and no magnetic resonance behavior is exhibited. Thus, by changing the polarization of the incoming linearly polarized EM wave (perpendicularly to the plane of the SRRs) one can easily identify the magnetic resonance regimes employing even a single layer of SRRs. This test was used by Enkrich et al.³⁰ to show that SRRs of linear size of about 220 nm created a negative μ frequency region centered at $\lambda = 1500$ nm.

In Fig.10 is shown a comparison of experimental and theoretical results regarding a LH transmission peak²⁸ of very high intensity. The LH nature of the peak was demonstrated by comparing the SRRs&wires system with a system of closed-SRRs&wires, using the approach described above.

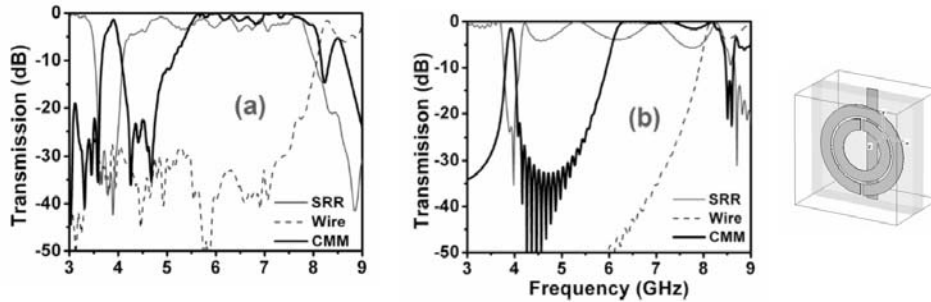


Fig. 10. In panel (a) the transmission coefficient vs. frequency through a left-handed slab of SRRs and wires is shown (solid-thick line) in the microwave range (the structure unit cell is shown at the right-side of the figure). Dashed line is the transmission for the wires-only system; it exhibits a plasma frequency at $f_p \approx 8$ GHz. The thin line is for SRRs only, showing a dip associated with negative μ at $f \approx 3.8$ GHz. When both wires and SRRs are combined (CMM) a LH peak at $f \approx 3.8$ GHz appears (thick line). Notice that the presence of SRR has lowered the plasma frequency to $f_p \approx 5$ GHz, as demonstrated in Fig. 9. Panel (b) presents the corresponding to panel (a) theoretical results, showing impressive agreement with the experimental data (no adjustable parameter enters the simulation). Figure is from Ref. 28. Copyright: Optical Society of America.

In Fig.11 we show experimental data and simulation results³¹ demonstrating the subwavelength resolution possibility (resolution of $\lambda/3$ in the figures) offered by metamaterials. The specific metamaterial is not a LH one but a photonic crystal, which shares several features³² with the LHMs, while it is inherently almost lossless.

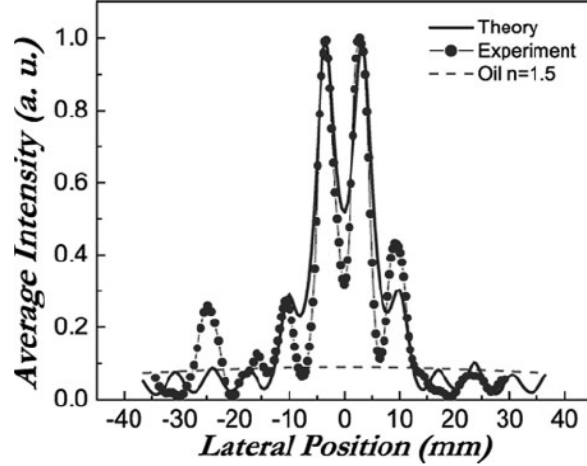


Fig. 11. Measured power distribution (solid points) and calculated average intensity (solid line) at 0.7 mm away from the second interface of a photonic crystal slab, for two incoherent sources at a distance $\lambda/3$. Figure from Ref. 31. Copyright: American Physical Society.

V. Goals and problems

In the microwave regime the existence and satisfactory performance of LHM has been established (see, e.g., Fig. 10 where losses less than 1 dB per cm have been achieved). The goal next is to push this kind of performance to higher frequencies all the way to the optical range (i.e., for $f \gtrsim 400\text{THz}$). There are two physical mechanisms which seem to block our path to this set goal. One is the increased role of the effective “kinetic” inductance, L_e (due to the kinetic energy of the current carrying electrons in the metal), and the other is the increased contribution of the ohmic losses in the metal. Both of them become more important as the resonance frequency is raised and the size of the unit cell is shrinking.

A rough analytical estimate of the frequency dependence of χ can be obtained for a system of periodically placed SRRs as follows: Let ℓ , w , t be the side length, the width, and the depth of each SRR (see Fig. 7 – single-gap SRR). The effective area, S , of the SRR is $S \simeq (\ell - w)^2$ and the volume of the primitive cell is $a \times a \times a_z = a^2 a_z$, where the direction z is normal to the plane of the SRR. An external field $B = \mu_o H$ along the z direction induces a current $I = i\omega SB/Z$ and a magnetic moment $m = IS$, where Z is the effective impedance $R - i(L\omega - 1/C\omega)$.

The magnetization M is by definition $m/a^2 a_z$ and the susceptibility $\chi = M/H$. Performing these simple calculations we find

$$\chi = -\frac{F\omega^2}{\omega^2 - \omega_o^2 + i(R/L)\omega}, \quad (20)$$

where F is a dimensionless number given by

$$F \simeq \pi(\ell - w)^3 \left[2a^2 a_z \left(\ln \frac{16(\ell - w)}{\pi b} - 1.5 \right) \left(1 + \frac{L_e}{L_m} \right) \right]^{-1}. \quad (21)$$

In obtaining (21) we have taken into account both contributions to the total inductance $L = L_m + L_e$, where L_m is the magnetic contribution and L_e is the kinetic energy contribution. We have also taken into account that³

$L_m \approx \left[4\mu_o(\ell-w)/2\pi \right] \left[\ln \frac{16(\ell-w)}{\pi b} - 1.5 \right]$, where $\pi b^2 \approx wt$. Setting typical values for $\ell = 0.8a$, $w = 0.1a$, $t = 0.05a$, $b = 0.04a$, $a_z = 0.2a$, we find that

$$F \approx \frac{1}{1 + (L_e/L_m)}. \quad (22)$$

The ratio R/L appearing in (20) can be estimated as follows

$$\frac{R}{L} = \frac{2\pi c^2}{\epsilon^{(o)} \omega_p^2 wt \tau} \frac{1}{\left(\ln \frac{16(\ell-w)}{\pi b} - 1.5 \right)} \frac{1}{\left(1 + \frac{L_e}{L_m} \right)}. \quad (23)$$

Setting the silver values, $\hbar\omega_p = 3.8\text{eV}$, $\epsilon^{(o)} = 6.6$, $\hbar/\tau = 0.04\text{eV}$, and geometrical dimensions as before, we find for $R\omega/L$ the following result:

$$\frac{R\omega}{L} \approx \frac{1}{6\pi\epsilon^{(o)}} \frac{\lambda_p^2}{wt} \frac{\omega_p\omega}{\omega_p\tau} \frac{1}{1 + \frac{L_e}{L_m}}, \quad (24)$$

where $\lambda_p \equiv 2\pi c/\omega_p \approx 326\text{nm}$ and $\omega_p\tau = 95$ for Ag. Thus, according to this rough estimate we have for Ag that

$$\frac{R}{L\omega_o} = 5.6 \times 10^{-4} \left(\lambda_p^2/wt \right) \left(\omega_p/\omega_o \right) \left(1 + \frac{L_e}{L_m} \right)^{-1}. \quad (25)$$

The ratio L_e/L_m is approximately $\lambda_p^2/6\pi\epsilon^{(o)}wt$ which shows that $L_e \approx L_m$ when $\lambda_p \approx \left(6\pi\epsilon^{(o)}wt \right)^{1/2} \approx 0.8a$, or when $a \approx 400\text{nm}$ for silver. In the limit of $a \ll 400\text{nm}$, the strength F of the resonance is

$$F \approx \frac{L_m}{L_e} \approx \frac{6\pi\epsilon^{(o)}wt}{\lambda_p^2} \approx 0.8 \frac{a^2}{\lambda_p^2}, \quad a \ll 3\lambda_p, \quad (26)$$

while the ratio $R/L\omega_o$ seems to approach $(\omega_p/\omega_o)(1/\omega_p\tau)$:

$$\frac{R}{L\omega_o} \approx \frac{\omega_p}{\omega_o} \frac{1}{\omega_p\tau} \approx \frac{\omega_p}{95\omega_o}, \quad a \ll 3\lambda_p, \quad (27)$$

where the last relation is appropriate for silver.

Eqs. (22) and (26) show the detrimental role of L_e which reduces the strength of the resonance from about one (when $a \gg 1\mu\text{m}$) to $0.8a^2/\lambda_p^2$ for $a \ll 3\lambda_p$, i.e., for ω_o reaching its saturation value as given by the formula in the caption of Fig. 7. Of course the existence of a non-zero R reduces the maximum value $|\text{Re}\chi|$ to less than one as a is decreased below a critical value; hence, the possibility of achieving negative values of μ at visible frequencies seems problematic, as shown in Fig. 12.

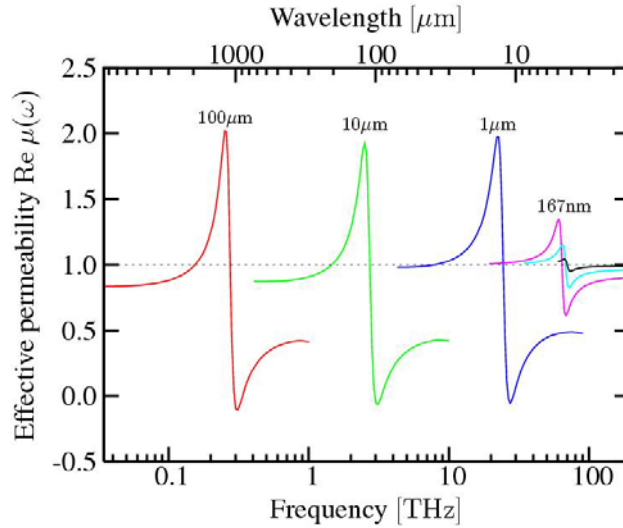


Fig. 12. Simulations showing the real part of the relative permeability for a single-ring single-gap SRR as the size of unit cell of the SRRs is reduced. Notice the drastic reduction of the strength of the resonance for unit cell sizes between $1 \mu\text{m}$ and 167nm . The metal is aluminum which is less favorable than silver. Figure from Ref. 17. Copyright: Wiley-VCH Verlag GmbH & Co. KGaA.

Of course there is always room for improvement by optimizing the details of the geometrical parameters and by choosing the most successful of the various designs. A recent paper by J. Zhou et al. (see Ref. 33) shows that by increasing the effective inductance to capacitance ratio, L/C , reduces the losses and increases the figure of merit. Furthermore, there are substantial differences among the various designs as far as the optimum performance is concerned^{34, 35}. This can be seen already from Fig. 7; it is shown also in Figs 13 and 14.

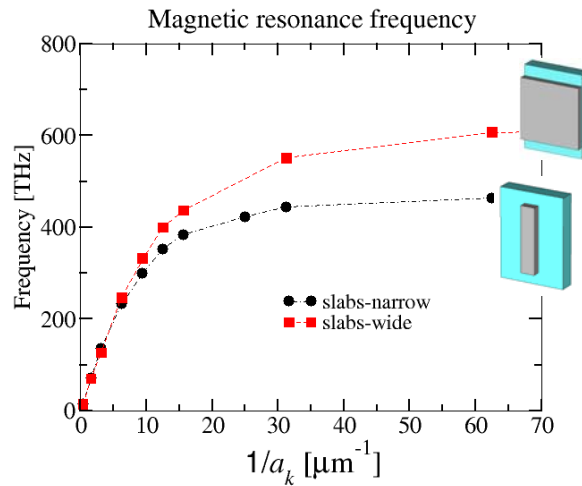


Fig. 13. Calculated magnetic resonance frequency as a function of the inverse unit cell size (along propagation direction), a_k , for systems of narrow and wide slab pairs. (Figure reports preliminary results concerning aluminum metallic slabs, with length $l=2.19a_k$, width $w=0.47a_k$ for the narrow slabs and $2.19a_k$ for the wide, thickness of the metal $t_m=0.25a_k$ and thickness of the substrate $t=0.5a_k$. The unit cell dimensions are $2.97a_k \times 2.19a_k \times a_k$.) Notice that only the widening of the slabs is able to push the magnetic resonance frequency much deeper in the visible range. Indeed, the system of wide slabs has been already used for the demonstration of resonant magnetic response throughout the entire visible range³⁶.

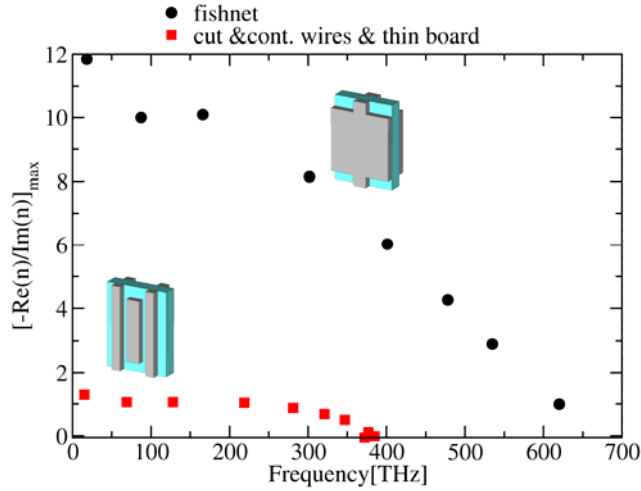


Fig. 14. Calculated optimum figure of merit ($FOM = -\text{Re}(n)/\text{Im}(n)$) vs. resonance frequency for the fishnet design and the design of narrow slabs and continuous wires. The fishnet design at the red end of the visible spectrum achieves a FOM of about 5.5.

Fig. 15, taken from Ref. 37, summarizes the progress towards achievement of optical negative permeability materials and left-handed materials up to 2007.

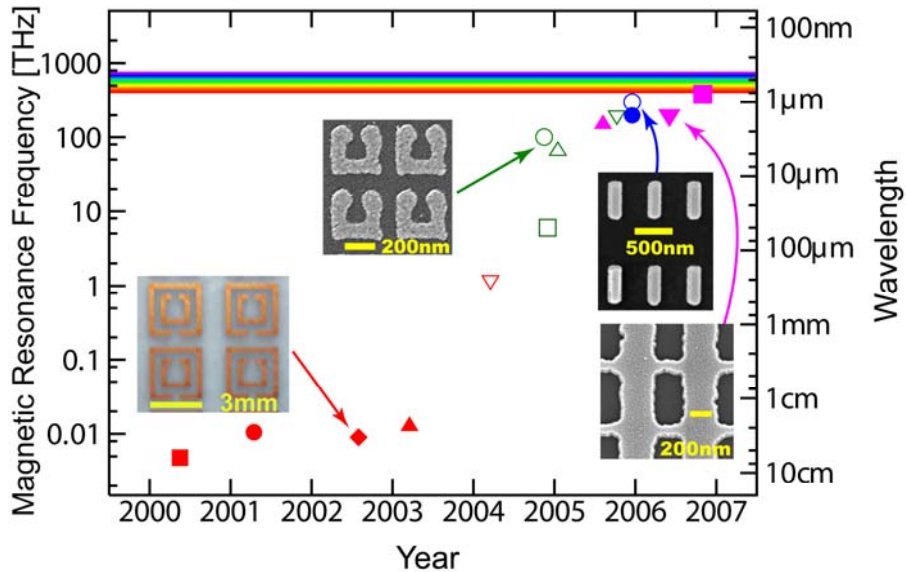


Fig. 15. Advances in scaling and redesigning metamaterials with artificial negative magnetic response and/or negative refractive index, n . The solid symbols denote structures with $n < 0$, while the open symbols structures with $\mu < 0$. The red color indicates structures based on the double split-ring resonator (SRR), the green color indicates single-ring SRRs, the blue pairs of metallic rods or slabs, and the magenta the "fishnet" structure. The four insets give pictures of fabricated structures in different frequency regions. Picture taken from Ref. 37. Copyright: AAAS.

VI. Summary

In this paper we have presented the basic concepts and some of the main results in a fast developing and exciting field which extends electromagnetism to new realms. This new field, which is less than ten years old, offers the possibility of several novel applications

which may revolutionize optics. It is based on artificial structures, consisting of elementary units (the so called “optical atoms”), the main feature of which is that both their effective permittivity and their effective permeability are negative over a common frequency range. This implies that the propagation of the phase of EM waves to be in the opposite direction than that of the energy of EM waves.

The existence and satisfactory performance of such metamaterials has been established in the GHz and low THz ranges and has been gradually extended to the red end of the visible spectrum, opening a novel era in optics. Two hurdles prevent for the time being the full exploitation of these so called optical left handed metamaterials (OLHMs). The first one is the increased amount of losses as we approach and enter the visible frequencies: The figure of merit (FOM), defined as the maximum value of $|\text{Re}n/\text{Im}n|$, does not exceed five or so (n is the index of refraction at the edge of the visible frequencies, $f \approx 400$ THz). The second is of practical nature and it has to do with the present day limited capabilities for fabricating complicated patterns at the nanoscale (unit cell size less than 100 nm). Actually, no true three-dimensional LHM has been fabricated yet at the nanoscale, although new fabrication methods³⁸ (such as direct laser writing³⁹ and nanoimprint lithography look promising). New improved designs adapted to existing fabrication capabilities may offer another path in overcoming this second hurdle.

Returning to the first, more basic hurdle, several approaches are tried, some of more obvious nature (such as design optimization, or development and employment of gain media exceeding present day performance) and other of more radical approach (such as a bottom up approach based on synthetic chemistry, proposed by some of the authors of this paper). A third possibility is to avoid this problem by focusing on thin film applications where losses are not of critical nature.

However, no researcher in the field expects that the intense research effort in the field, focused on these two hurdles, will diminish, if for no other reason, but for the numerous and exciting applications waiting to be realized. Among them we mention: Optical switching and bistability, zero reflectance, modulators (employing chiral OLHMs), strong diamagnetic response (magnetic levitation), zero index of refraction structures as beam collimators and, of course, superlenses and hyperlenses^{40, 41}, based on the exploitation of the evanescent waves. Superlenses are capable of beating the diffraction limit at near field, by amplifying the evanescent waves, while hyperlenses aim at converting evanescent waves to propagating waves (through mainly the use of anisotropic materials with hyperbolic dispersion).

Acknowledgements: Authors would like to acknowledge financial support by EU under the projects Metamorphose, PHOREMOST, Molecular Imaging (LSHG-CT-2003-503259), PHOME (FET Contract No. 213390), ENSEMBLE, ECONAM, and the COST Actions MP0702 and MP0803, by the US Department of Energy (Basic Energy Sciences) under Contract No. DE-AC02-07CH11358, by the AFOSR under MURI grant (FA9550-06-1-0337), by DARPA (Contract No. MDA-972-01-2-0016), by Office of Naval Research (Award No. N00014-07-1-0359), and by the Air Force Office of Scientific Research, Air Force Material Command, USAF (Grant No. FA8655-07-1-3037).

References

1. N. W. Ashcroft and N. D. Mermin, *Solid State Physics*, (Thomson Learning, Inc. 1976).
2. D. J. Griffiths, *Introduction to Electrodynamics*, 2nd ed. (Prentice Hall, 1996).
3. L. D. Landau and E. M. Lifshiz, *Electrodynamics of Continuous Media*, 2nd ed. (Pergamon Press, Oxford, 1984).

4. E. N. Economou, "The Physics of Solids", to be published by Springer-Verlag.
5. V. G. Veselago, *Sov. Phys. Usp.* 10, 509-514 (1968).
6. R. W. Ziolkowski and E. Heyman, *Phys. Rev. E* 64, 056625 (2001).
7. J. B. Pendry, *Phys. Rev. Lett.* 85, 3966 (2000).
8. A. Ramakrishna, and J. B. Pendry, *Appl. Phys. Lett.* 82, 1506–1508 (2003).
9. Th. Koschny, R. Moussa and C. M. Soukoulis, *J. Opt. Soc. Am. B* 23, 485 (2006).
10. D. R. Smith, Willie J. Padilla, D. C. Vier, S. C. Nemat-Nasser and S. Schultz, *Phys. Rev. Lett.* 84, 4184 (2000).
11. J. B. Pendry, A. T. Holden, W.J. Stewart and I. Youngs, *Phys. Rev. Lett.* 25, 4773 (1996); J. B. Pendry, A. J. Holden, D. J. Robbins, and W. J. Stewart, *J. Phys. Cond. Matt.* 10, 4785 (1998).
12. J. B. Pendry, A. Holden, D. Robbins, and W. Stewart, *IEEE Trans. Microwave Theory Tech.* 47, 2075 (1999).
13. For review see at C. M. Soukoulis, M. Kafesaki and E. N. Economou, "Negative index materials: New frontiers in optics," *Adv. Mater.* 18, 1941 (2006).
14. K. Aydin, I. Bulu, K. Guven, M. Kafesaki, C. M. Soukoulis, E. Ozbay, *New Journal of Physics* 7, 168 (2005).
15. J. Zhou, Th. Koschny, M. Kafesaki, E. N. Economou, J. B. Pendry, and C. M. Soukoulis, *Phys. Rev. Lett.* 95, 223902 (2006).
16. L. Solymar, *Lectures on Electromagnetic Theory* (Oxford University Press, Oxford, 1976).
17. C. M. Soukoulis, Th. Koschny, J. Zhou, M. Kafesaki, E. N. Economou, *Phys. Stat. Sol. (b)* 244, 1181 (2007).
18. M. W. Klein, C. Enkrich, M. Wegener, C. M. Soukoulis, and S. Linden, *Opt. Lett.* 31, 1259 (2006).
19. J. Zhou, E. N. Economou, Th. Koschny, and C. M. Soukoulis, *Opt. Lett.* 31, 3620 (2006).
20. S. Zhang, W. Fan, N. C. Panoiu, K. J. Malloy, R. M. Osgood, and S. R. J. Brueck, *Phys. Rev. Lett.* 95, 137404 (2005); S. Zhang, W. Fan, B. K. Minhas, A. Frauenglass, K. J. Malloy, and S. R. J. Brueck, *Phys. Rev. Lett.* 94, 37402 (2005).
21. R. Ulrich, *Infrared Phys.* 7, 37 (1967).
22. M. Kafesaki, I. Tsiapa, N. Katsarakis, Th. Koschny, C. M. Soukoulis and E. N. Economou, *Phys. Rev. B* 75, 235114 (2007).
23. T. Koschny, M. Kafesaki, E. N. Economou, and C. M. Soukoulis, *Phys. Rev. Lett.* 93, 107402 (2004).
24. M. Kafesaki, Th. Koschny, J. Zhou, N. Katsarakis, I. Tsiapa, E. N. Economou and C. M. Soukoulis, *Physica B: Cond. Matt.* 394, 148 (2007).
25. R. Shelby, D. R. Smith and S. Schultz, *Science* 292, 77 (2001).
26. Ekmel Ozbay, Koray Aydin, *Photon. and Nanostr.* 6, 108 (2008).
27. J. Valentine, S. Zhang, Th. Zentgraf, E. Ulin-Avila, D. A. Genov, G. Bartal and Xiang Zhang, *Nature* (2008) – available online.
28. K. Aydin, K. Guven, Lei Zhang, M. Kafesaki, C. M. Soukoulis, and E. Ozbay, *Optics Letters* 29, 2623 (2004).
29. N. Katsarakis, T. Koschny, M. Kafesaki, E. N. Economou and C. M. Soukoulis, *Appl. Phys. Lett.* 84, 2943 (2004).
30. C. Enkrich, S. Linden, M. Wegener, S. Burger, L. Zswehdreich, F. Schmidt, J. Zhou, T. Koschny and C. M. Soukoulis, "Magnetic metamaterials at telecommunication and visible frequencies", *Phys. Rev. Lett.* 95, 203901 (2005).
31. E. Cubukcu, K. Aydin, E. Ozbay, S. Foteinopoulou and C. M. Soukoulis, *Phys. Rev. Lett.* 91, 207401 (2003).
32. S. Foteinopoulou, E. N. Economou and C. M. Soukoulis, *Phys. Rev. Lett.* 90, 107402 (2003).
33. J. Zhou, Th. Koschny, C. M. Soukoulis, *Opt. Expr.* 16, 11147 (2008).
34. G. Dolling, M. Wegener, C. M. Soukoulis and S. Linden, *Opt. Expr.* 15, 1153 (2007).
35. M. Kafesaki, Th. Koschny, C. M. Soukoulis, and E. N. Economou, "Designing one-, two and three-dimensional left-handed materials", Chapter in "Handbook of Artificial

Electromagnetic Materials", edited by F. Capolino (Taylor & Francis, to appear in December 2008).

36. W. Cai, U. K. Chettiar, H.-K. Yuan, V. C. de Silva, A. V. Kildishev, V. P. Drachev, and V. M. Shalaev, *Opt. Expr.* 15, 3333 (2007).
37. C. M. Soukoulis, S. Linden, and M. Wegener, *Science* 315, 47 (2007).
38. A. Boltasseva and V. M. Shalaev, *Metamaterials* 2, 1 (2008).
39. M. S. Rill, C. Plet, M. Thiel, I. Staude, G. von Freymann, S. Linden, and M. Wegener, *Nature Mater.* 7, 543 (2008).
40. Z. Liu, H. Lee, Y. Xiong, Ch. Sun, X. Zhang, *Science* 315, 1686 (2008).
41. Z. Jacob, L. V. Alekseyev, E. Narimanov, *Opt. Express* 14, 8247 (2006).

Authors' CVs

Prof. E. N. Economou obtained his Ph.D. in 1969 at the Physics Department of the University of Chicago. Before joining the University of Crete as a Professor, in 1981, he was a Professor at University of Virginia. From 1983 to 2003 he served as president of FORTH. He has a strong research effort on the properties of disordered systems, high T_c superconductors and amorphous semiconductors, and wave propagation in random media. His recent work on electromagnetic and elastic wave propagation is well received, since he has given talks as an invited speaker in a number of international conferences. He has 230 publications in refereed journals and he has been cited more than 6000 times in SCI journals. He is the author of the book *Green's Function in Quantum Physics* and of six physics texts in Greek. He is a fellow of the American Physical Society and has received many distinctions, among them the Descartes award for collaborative research on left-handed materials in 2005.

Dr. Maria Kafesaki is a researcher at the Theoretical and Computational Division of the IESL-FORTH. She obtained her Ph.D. in 1997, at the Physics Department of the University of Crete, Greece. She has worked as post-doctoral researcher in the Consejo Superior de Investigaciones Cientificas in Madrid, Spain, and in IESL of FORTH. Her research is on the area of electromagnetic, and elastic wave propagation in periodic and random media, with emphasis on photonic crystals, and left-handed materials, where she has a long time theoretical and computational experience. She has around 45 publications in refereed journals and conference proceedings.

Dr. Thomas Koschny, received his M.Sc. and Ph.D. degrees in physics from the University of Leipzig, Germany, in 1997 and 2001, respectively. During 2000-2002, he worked as a post-doctoral researcher on Quantum Hall Effect at the Physikalisch-Technische Bundesanstalt Braunschweig (PTB), Germany. Since 2003 he is working on electromagnetic wave propagation in left-handed metamaterials at Institute of Electronic Structure and Laser (IESL), Foundation for Research and Technology Hellas (FORTH), Crete, Greece. Since 2004 he is a researcher at Ames Laboratory and Department of Physics and Astronomy at Iowa State University, Iowa, USA. His current research interests include theory of metamaterials and photonic crystals

Prof. C. M. Soukoulis obtained his Ph.D. in 1978 at the Physics Department of University of Chicago. He is currently a senior scientist at FORTH and Distinguished Professor of Physics at Iowa State University. He is a Fellow of the APS, OSA and AAAS. He has more than 300 publications in refereed journals and he has given more than 150 invited talks. His work on photonic band gaps (PBG), random lasers and left-handed materials is well known and well received. He has organized three NATO ASI on PBGs and he was the director of PECS-VI that took place in Crete in June 2005. He also has three patents concerning the potential applications of the photonic band gaps and left-handed materials. He recently received the Senior Humboldt Research Award. He has been cited ~10000 times in SCI journals.